CANCER DIAGNOSIS & PROGNOSIS
3: 282-290 (2023) doi: 10.21873/cdp.10213

Review

Spindle Cell Lipoma and Pleomorphic Lipoma: An Update and Review

YUKIKO OHSHIMA[1*], JUN NISHIO[2*], SHIZUHIDE NAKAYAMA[1], KAORI KOGA[3], MIKIKO AOKI[3] and TAKUAKI YAMAMOTO[1]

[1]*Department of Orthopaedic Surgery, Faculty of Medicine, Fukuoka University, Fukuoka, Japan;*
[2]*Section of Orthopaedic Surgery, Department of Medicine, Fukuoka Dental College, Fukuoka, Japan;*
[3]*Department of Pathology, Faculty of Medicine, Fukuoka University, Fukuoka, Japan*

Abstract. *Spindle cell lipoma (SCL) is a benign adipocytic tumor that primarily occurs in the subcutis of the posterior neck, upper back, and shoulder, particularly of middle-aged males. SCL and pleomorphic lipoma (PL) represent a morphological spectrum of one disease process. The lesion typically presents as a relatively small (<5 cm), mobile, slow-growing, painless mass. Magnetic resonance imaging reveals the lesion to be a well-defined subcutaneous mass with a mixture of adipose and non-adipose components. Intense enhancement of the non-adipose component is seen after contrast administration. Histologically, SCL is composed of variable distributions of mature adipocytes, bland spindle cells and ropey collagen bundles and PL also contains pleomorphic and multinucleated floret-like giant cells. By immunohistochemistry, the spindle and pleomorphic/floret-like giant cells of SCL/PL are diffusely positive for CD34 and show loss of nuclear RB transcriptional corepressor 1 (RB1) expression. Recent cytogenetic and molecular genetic studies have shown heterozygous deletions of 13q14, including the RB1 gene. SCL/PL can be successfully treated with simple excision, with a very low recurrence rate. Knowledge of these peculiar tumors is important because it can mimic a variety of benign and malignant soft-tissue tumors. This review provides an updated overview of the clinical, radiological, histopathological, cytogenetic, and molecular genetic features of SCL/PL.*

*These Authors contributed equally to this study.

Correspondence to: Jun Nishio, MD, Ph.D., Section of Orthopaedic Surgery, Department of Medicine, Fukuoka Dental College, 2-15-1 Tamura, Sawara-ku, Fukuoka 814-0193, Japan. Tel: +81 928010411, Fax: +81 928010735, e-mail: nishio@fdcnet.ac.jp

Key Words: Spindle cell lipoma, pleomorphic lipoma, RB1, cytogenetics, atypical lipomatous tumor, atypical spindle cell/pleomorphic tumor, review.

Spindle cell lipoma (SCL) is a relatively rare, benign adipocytic tumor composed of a variable mixture of mature adipocytes, bland spindle cells and ropey collagen bundles. Pleomorphic lipoma (PL) lies on a morphological spectrum with SCL and is characterized by pleomorphic spindle cells and multinucleated floret-like giant cells (1). The etiology of SCL/PL remains unknown. SCL/PL can show a morphological overlap with a variety of soft-tissue tumors, including atypical spindle cell/pleomorphic lipomatous tumor (ASCPLT), atypical lipomatous tumor (ALT), solitary fibrous tumor (SFT), myxoid liposarcoma (MLS) and dedifferentiated liposarcoma (DDLS). In our opinion and experience, the imaging appearance of SCL/PL is not pathognomonic and reflects the histological composition of the lesion which contains variable amounts of adipose and non-adipose tissue. Advances in knowledge of the imaging, histopathology and genetics of SCL/PL are leading to more accurate diagnosis and appropriate treatment. This review highlights the clinical, radiological, histological, immuno-histochemical, cytogenetic and molecular genetic features of SCL/PL. In addition, we will discuss the differential diagnosis of SCL/PL.

Clinical Features

SCL/PL can occur at any age but has a peak incidence in the fifth to seventh decades of life, with a marked male predominance (approximately 90%) (1). It typically presents as a solitary, mobile, slow-growing, painless, subcutaneous

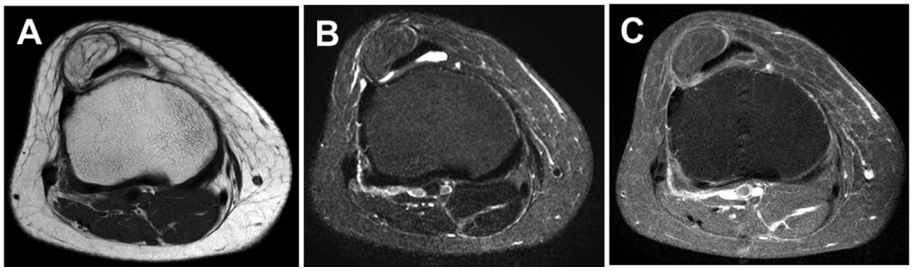

Figure 1. *A 56-year-old woman with spindle cell lipoma in the right knee. Axial T1-weighted (A), T2-weighted fat-suppressed (B) and contrast-enhanced fat-suppressed T1-weighted (C) images showing a well-defined, predominantly fatty mass with scattered, thin septae.*

mass in the posterior neck, upper back, and shoulder (shawl distribution). Occasional lesions are multifocal or arise in a familial setting (2). Fascial and skeletal muscle involvement is uncommon. In women, SCL is more likely to occur outside the shawl distribution and in a younger age group (3). The diameter ranges from 1.0 to 14.0 cm (usually less than 5 cm) (4). Simple excision is the treatment of choice and prognosis is excellent. There is no metastatic potential and no reports of malignant transformation.

Radiological Features

Various imaging modalities have been applied for the detection of SCL/PL. Although identification of fat within the lesion is the most important clue to make diagnosis of adipocytic tumors on imaging, it is recognized that SCL/PL may have minimal or no visible fat. It is essential to be familiar with the key imaging features of SCL/PL to avoid an unnecessary radical surgery.

Radiographs may be unremarkable or reveal a soft-tissue mass depending on the size and location of the lesion. Although cases of bone erosion have been described (5, 6), the underlying bone is typically normal. Ultrasound shows non-specific soft-tissue echogenicity with moderate internal Doppler vascularity in the non-adipose component (7). Computed tomography (CT) reveals a well-defined soft-tissue mass with slightly increased attenuation compared with that of subcutaneous fat in the adipose component and slightly low attenuation compared with that of skeletal muscle in the non-adipose component (8). Contrast-enhanced CT demonstrates significant enhancement in the non-adipose component (7-10). In our experience, the non-adipose component is best detected and evaluated with magnetic resonance imaging (MRI). On MRI, the lesion is usually well-defined and contains variable amounts of adipose and non-adipose components (7-12) (Figure 1). In general, many lesions contain between 25% and 75% fat (10). However, a significant number of SCL/PLs may exhibit a "low-fat" or "fat-free" appearance that can mimic more aggressive tumors such as MLS, DDLS and non-adipocytic sarcomas (7, 11, 12). The non-adipose component displays isointense relative to skeletal muscle on T1-weighted images and variable signal intensity on T2-weighted images. Contrast-enhanced MRI demonstrates intense enhancement in the non-adipose component (10, 12). Recently, Kawaguchi *et al*. reported that the maximum diameter, the proportion of non-adipose area on T1-weighted images and solid hyperintense area on fat-suppressed T2-weighted images were useful MRI features for differentiating SCL/PL from ALT (13). To date, position-emission tomography (PET) features for SCL/PL have been described in only three cases (7). Integrated PET/CT images show increased uptake in the non-adipose component, with a standardized uptake value (SUV) range of 2.0-8.0. In our opinion, SCL/PL should be considered a possible diagnosis when a well-defined, complex, fatty mass is encountered in the subcutis of a middle-aged man.

Histological and Immunohistochemical Characteristics

Grossly, SCL/PL appears as an oval or discoid, well-circumscribed mass with a yellow or grayish white cut surface (1). Histologically, SCL is composed of variable distributions of mature adipocytes, bland spindle cells and ropey collagen bundles (Figure 2). The ratio of the spindle cells and mature adipocytes is variable, but the great majority of cases have significant amounts of both components. In the other end of the spectrum, PL is characterized by the presence of pleomorphic spindle cells and multinucleated floret-like giant cells. Occasional lipoblasts can be present in a significant subset of cases (14). Mitotic figures are rare, and necrosis is absent. There is relatively sparse vascularity, of small to medium-sized thick-walled, sometimes hyalinized vessels. A variety of variants of SCL have been described including low-fat, fat-free, (pseudo)angiomatous, fibrous, myxoid and plexiform subtypes (1, 15-19). Immunohistochemically, the spindle, pleomorphic and multinucleated floret-like cells are diffusely positive for CD34 (Figure 3) and show loss of nuclear RB transcriptional corepressor 1 (RB1) protein expression (20). Immunostainings for S-100 protein, desmin and smooth muscle actin (SMA) are typically negative.

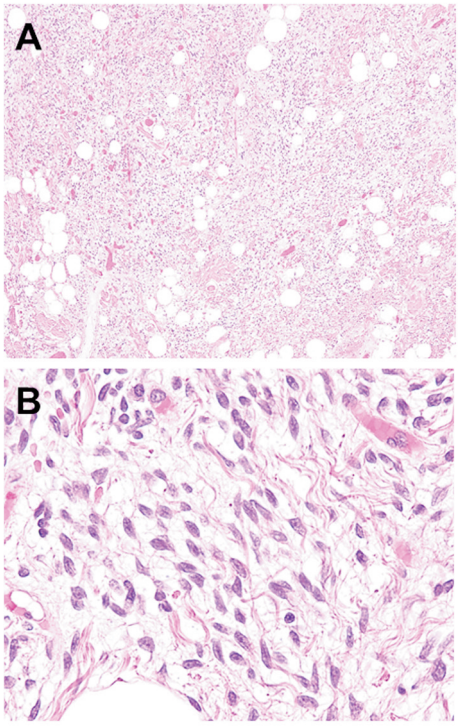

Figure 2. *Histological features of spindle cell lipoma. (A) The tumor is composed of mature adipocytes, spindle cells and ropey collagen bundles in a fibromyxoid stroma (hematoxylin and eosin staining, original magnification ×100). (B) The spindle cells are bland and lack nuclear hyperchromasia and cytological atypia (hematoxylin and eosin staining, original magnification ×200).*

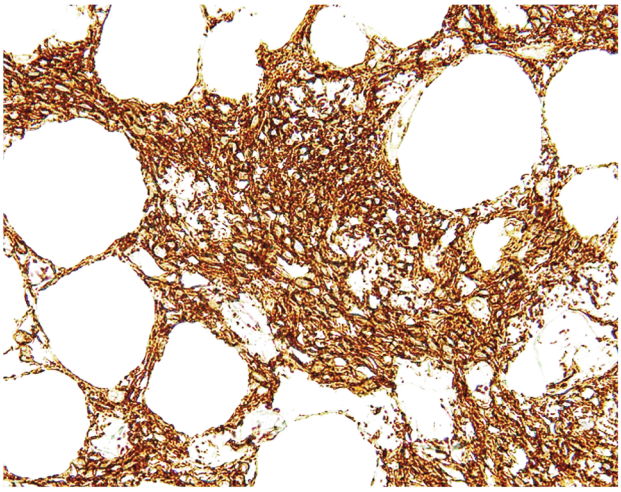

Figure 3. *Immunohistochemical features of spindle cell lipoma. The spindle cells are diffusely and strongly positive for CD34 (original magnification ×200).*

Cytogenetic and Molecular Genetic Features

SCL and PL show similar cytogenetic aberrations which are usually more complex than conventional lipoma (21). SCL/PL displays unbalanced karyotypes, mostly hypodiploid, with multiple partial losses. Structural rearrangements, mainly deletions, of chromosome arm 13q or losses of whole chromosome 13 are the most common cytogenetic aberrations (22). The related region (13q14) contains the *RB1* gene. Fluorescence *in situ* hybridization (FISH) analyses have revealed a heterozygous deletion of *RB1* in a subset of SCL/PLs (22, 23). Single nucleotide polymorphism array analyses have identified two minimally deleted regions in 13q14 in SCL (24). The first region includes *RB1*, lysophosphatidic acid receptor 6 (*LPAR6*), RCC1 and BTB domain containing protein 2 (*RCBTB2*) and cysteinyl leukotriene receptor 2 (*CYSLTR2*). The second region lies between the genes fibronectin type III domain containing 3A (*FNDC3A*) and transmembrane phosphoinositide 3-phosphatase and tensin homolog 2 pseudogene 3 (*TPTE2P3*, formerly *LOC220115*) and harbors 34 genes including SPRY domain containing 7 (*SPRDY7*, formerly *C13orf1*), dehydrogenase/reductase 12 (*DHRS12*), ATPase copper transporting beta (*ATP7B*), ALG11 alpha-1,2-mannosyltransferase (*ALG11*) and vacuolar protein sorting 36 homolog (*VPS36*) and the two microRNA genes *miR-15a* and *miR-16-1*. Recently, Uehara *et al*. reported that SCL/PL expressed decreased levels of forkhead box O1 (FOXO1) and RB1 and showed the activation of p38 mitogen-activated protein kinase (MAPK) pathway induced by oxidative stress (25). In addition to 13q deletions, SCL/PL also shows chromosome 16q losses with partial monosomy (26). The involved genes have not been specifically identified in this region. In our extensive experience, SCL/PL lacks amplification of murine double minute 2 (*MDM2*).

Deletion of *RB1* is shared with a group of morphologically similar spindle cell tumors with variable admixed fat and immunohistochemically overlapping features, including SCL/PL, ASCPLT, mammary-type myofibroblastoma and cellular angiofibroma (CAF) (27). *RB1* loss has also been described as a recurrent finding in other mesenchymal neoplasms such as pleomorphic fibroma (28) and superficial acral fibromyxoma (29). The current World Health Organization classification of soft-tissue tumors suggests that these lesions are typically benign and are mainly seen in the older adult population. It is of interest that RB1 has been implicated in the regulation of adipocyte differentiation (30, 31).

Differential Diagnosis

The differential diagnosis for SCL/PL is broad due to its varying morphology and includes benign, intermediate, and malignant soft-tissue tumors such as ASCPLT, CAF, ALT, fat-forming SFT, MLS and DDLS (Table I).

ASCPLT is a new entity of benign adipocytic neoplasm that usually presents as an enlarging or persistent mass in the extremities and limb girdles, sometimes with tenderness. It can occur at any age but has a peak incidence in the sixth decade of life, with a slight male predominance. The diameter ranges from 0.5 to 28.0 cm (32). ASCPLT has a low rate of non-destructive local recurrence (10-15%) (32). Importantly, there is no risk for dedifferentiation or metastasis. There is only limited description of the imaging appearance of ASCPLT (33-35). On MRI, the lesion displays variable signal intensity on T1- and T2-weighted images. ASCPLT and SCL/PL tend to have similar enhancement patterns on T1-weighted images (33). Preoperative imaging diagnosis is difficult, and histopathological and molecular evaluations are required for a definite diagnosis. Histologically, ASCPLT shows infiltrative margins and demonstrates atypical hyperchromatic spindle cells, pleomorphic lipoblasts and bizarre pleomorphic (multinucleated) cells with mitotic activity in contrast with SCL/PL. ASCPLT typically lacks ropey collagen bundles. ASCPLT and SCL/PL share similar immunohistochemical features such as CD34 positivity and loss of RB1 protein expression (50-70%) (32). In addition, ASCPLT shows variable expression of S100 protein and desmin. Weak and/or focal expression of MDM2 or cyclin-dependent kinase 4 (CDK4) may be seen, but the combination of MDM2 and CDK4 expression is not compatible with a diagnosis of ASCPLT (36). Molecular studies have shown that deletions of 13q14 in ASCPLT are more extensive and complex than in SCL/PL, including multiple functionally important exons of *RB1* and its adjacent genes *RCBTB2*, deleted in lymphocytic leukemia 1 (*DLEU1*) and integral membrane protein 2B (*ITM2B*) (37). Moreover, monosomy 7 has been described in a subset of ASCPLTs (36, 38). *MDM2* or *CDK4* amplification is absent in ASCPLT.

CAF is a benign fibroblastic tumor that usually presents as a slow-growing, painless, subcutaneous mass in the vulvovaginal region for women and the inguinoscrotal region for men. It has a peak incidence in the fifth decade of life in women and the seventh in men, with no sex predilection. The diameter ranges from 0.6 to 25.0 cm (39). Simple excision is the treatment of choice and local recurrence is uncommon. On MRI, the lesion is well-defined and displays intermediate or low signal intensity on T1-weighted images and heterogeneous high signal intensity on T2-weighted images (40). Contrast-enhanced MRI demonstrates intense heterogeneous enhancement. The presence of intralesional fat has been reported in up to 56% of CAF (41). CAF has some morphological overlap with SCL/PL. Histologically, the lesion consists of uniform, short spindle-shaped cells in an edematous to fibrous stroma. Mature adipocytes are observed in close to 50% of cases (39). In contrast with SCL/PL, there are numerous small to medium-sized thick-walled blood vessels, often with perivascular fibrosis or hyalinization. CAF and SCL/PL share similar immunohistochemical features such as CD34 positivity (30-60%) and loss of RB1 protein expression (39). Moreover, CAF shows expression for estrogen receptor and progesterone receptor (42). Variable expression of SMA and desmin is seen in a minority of cases (39). Genetically, loss of 13q14, including *RB1*, is characteristic of CAF as well as SCL/PL (27, 43-46).

ALT is an intermediate (locally aggressive) mesenchymal neoplasm that usually presents as a deep-seated, painless mass in the lower extremities, trunk, and retroperitoneum. It most commonly occurs in middle-aged and older adults, with no sex predilection (47). Unlike SCL/PL, ALT shows a significant propensity for local recurrence and can dedifferentiate to DDLS (incidence up to 10%) (48). Radiographs may depict the presence of a soft-tissue mass. Calcification is seen in 10-32% of cases (49). Ultrasound reveals a heterogeneous, multilobulated, typically well-defined mass. The presence of hyperechoic foci suggests fat (49). On CT and MRI, ALT shows a predominantly adipose mass with irregularly thickened, linear, swirled and/or nodular septa. Generally, the lesion contains at least 75% adipose tissue (49). In our experience, the non-adipose component displays non-specific decreased signal intensity on T1-weighted images and variably increased signal intensity on T2-weighted images. Contrast-enhanced MRI usually demonstrates significant enhancement in the non-adipose component (50). Histologically, ALT may be indistinguishable from fat-rich SCL/PL. However, the spindle cells seen in ALT contain more irregular, enlarged, hyperchromatic nuclei. In contrast to SCL/PL, ALT usually lacks ropey collagen bundles. Immunohistochemically, nuclear expression of MDM2 and/or CDK4 is seen in most cases (47). Unlike SCL/PL, ALT is cytogenetically characterized by the presence of one or more supernumerary ring and/or giant marker chromosomes containing amplified chromosome 12 sequences (21). Moreover, *MDM2* and/or *CDK4* amplification is present in ALT. Detection of *MDM2* (and/or *CDK4*) amplification by fluorescence in situ hybridization (FISH) serves to distinguish ALT from SCL/PL.

SFT is an intermediate (rarely metastasizing) mesenchymal neoplasm that usually presents as a slow-growing, painless mass in the pleura, abdominal cavity, extremities and head and neck. It most commonly occurs in middle-aged adults, with no sex predilection (51). Wide excision is the current treatment mainstay. Local recurrence occurs in 10-40% of cases and distant metastases develop in up to 35-45% of cases (51, 52). Dedifferentiation can occur at the end of the transforming histological stage of SFT. Radiographs may reveal a non-specific soft-tissue mass. Calcification is rare, occurring in about 9% of cases (53). Ultrasound generally shows a heterogeneous, well-defined, hypoechoic mass (54). CT reveals a well-defined,

Table I. *Differential diagnosis of spindle cell/pleomorphic lipoma.*

Entity	Clinical features	Histological and immunohistochemical features	Molecular features
SCL/PL	Fifth to seventh decades; Male predominance. Most cases occur in the subcutaneous tissue of the posterior neck, upper back, and shoulder.	Well-defined lesion, composed of mature adipocytes, bland spindle cells and ropey collagen bundles. Pleomorphic spindle cells and multinucleated floret-like giant cells are present in PL. CD34+; SMA-; desmin-; RB1-; MDM2-; CDK4-.	Deletion of 13q14; *RB1* deletion; no amplification of *MDM2* or CDK4.
ASCPLT	Sixth decade; Male predominance. Many cases occur in the subcutaneous tissue of the limbs, limb girdles and extremities.	Ill-defined lesion, composed of atypical hyperchromatic spindle cells, pleomorphic lipoblasts, and bizarre pleomorphic cells. CD34+; desmin+; S-100 protein+; RB1-; MDM2-; CDK4-.	Deletion of 13q14; *RB1* deletion; no amplification of *MDM2* or *CDK4*.
CAF	Fifth decade; Female predominance. Most cases occur in the subcutaneous tissue of the vulvovaginal region.	Well-defined lesion; composed of bland spindle cells in an edematous to fibrous stroma. Mature adipocytes are seen in close to 50% of cases. Numerous small to medium-sized thick-walled blood vessels are present. CD34+; ER+; PR+; RB1–; MDM2–; CDK4–.	Deletion of 13q14; RB1 deletion; no amplification of *MDM2* or *CDK4*.
ALT	Fourth to sixth decades; Equal male and female incidence. Most cases occur in the deep soft tissue of the lower extremities and trunk. The retroperitoneum is also commonly involved.	Well-defined lesion, composed of mature adipocytes with a significant variation in size and a variable number of lipoblasts. Atypical, hyperchromatic stromal cells are identified. CD34-; desmin-; RB1+; MDM2+; CDK4+.	Ring or giant marker chromosomes; amplification of *MDM2* and *CDK4*.
SFT	Fifth to seventh decades; Equal male and female incidence. Most cases occur in the deep soft tissue of the extremities and head and neck. The pleural and abdominal cavities are also commonly involved.	Well-defined lesion, composed of ovoid to spindle-shaped cells with a patternless architecture embedded in a variably collagenous stroma. Branching and hyalinized staghorn-like blood vessels are present. CD34+; CD99+; BCL2+; STAT6+; RB1+; MDM2–; CDK4–.	*NAB2-STAT6* fusion; no amplification of *MDM2* or *CDK4*.
MLS	Fourth to fifth decades; Equal male and female incidence. Most cases occur in the deep soft tissue of the proximal lower extremities.	Well-defined lesion, composed of ovoid cells and a variable number of small lipoblasts in a prominent myxoid stroma. A delicate, arborizing capillary vascular network is seen. CD34–; DDIT3+; RB1+; MDM2–; CDK4–.	*FUS-DDIT3* fusion or *EWSR1-DDIT3* fusion; no amplification of *MDM2* or *CDK4*.
DDLS	Sixth to seventh decades; Equal male and female incidence. Most cases occur in the deep soft tissue of the extremities. The retroperitoneum and paratesticular regions are also commonly involved.	Well-defined lesion, composed of a coexistence of ALT and non-adipose (dedifferentiated) components. A varying number of monovacuolated or multivacuolated lipoblasts are seen. CD34+ (variable); SMA+ (focal); desmin+ (focal); RB1+; MDM2+; CDK4+.	Ring or giant marker chromosomes; high-level amplification of 1p32 and 6q23; amplification of *MDM2* and *CDK4*.

ALT: Atypical lipomatous tumor; ASCPLT: atypical spindle cell/pleomorphic lipomatous tumor; CAF: cellular angiofibroma; CDK4: cyclin-dependent kinase 4; DDIT3: DNA damage-inducible transcript 3; DDLS: dedifferentiated liposarcoma; ER: estrogen receptor; EWSR1: EWS RNA binding protein 1; FUS: FUS RNA binding protein; MDM2: murine double minute 2; MLS: myxoid liposarcoma; NAB2: NGFI-A binding protein 2; PR: progesterone receptor; RB1: RB transcriptional corepressor 1; SCL/PL: spindle cell/pleomorphic lipoma; SFT: solitary fibrous tumor; SMA: smooth muscle actin; STAT6: signal transducer and activator of transcription 6.

occasionally lobulated mass of similar attenuation to that of skeletal muscle. Contrast-enhanced CT demonstrates mild to marked heterogeneous enhancement (54). On MRI, the lesion is well-defined and displays isointense signal intensity on T1-weighted images and variable signal intensity on T2-weighted images (55). Contrast-enhanced MRI demonstrates strong focal or diffuse enhancement. In our experience, the presence of prominent collateral feeding vessels is a useful distinguishing imaging feature of SFT. Histologically, the lesion consists of uniform ovoid to spindle-shaped cells with a patternless architecture embedded in a variably collagenous stroma. Some SFTs contain a component of mature adipose tissue (56). This SFT variant (fat-forming SFT) can be confused with SCL/PL. In contrast with SCL/PL, SFT typically contains branching and hyalinized staghorn-like blood vessels. Immunohistochemically, SFT typically shows diffuse expression of CD34, CD99 and BCL2 (57). Importantly, immunostaining for signal transducer and activator of transcription 6 (STAT6) reliably distinguishes SFT from SCL/PL (58). The discovery of a NGFI-A binding

protein 2 (*NAB2*)-*STAT6* fusion gene has recently led to more precise diagnosis of SFT (59). Unlike SCL/PL, SFT is not characterized by deletion of *RB1* and corresponding nuclear loss of expression for RB1 (20, 60).

MLS is a malignant adipocytic neoplasm that typically presents as a large, painless mass in the proximal lower extremities. It has a peak incidence in the fourth to fifth decades of life, with no sex predilection (61). Wide excision with or without radiotherapy is the treatment of choice. Local recurrence occurs in 12-25% of cases and distant metastases develop in about 30-60% of cases (61). The presence of a round cell component is associated with a significant higher rate of metastasis and an overall adverse outcome. Unlike other soft-tissue sarcomas, MLS shows a high incidence of extrapulmonary metastasis to the soft tissues and bones. Radiographs may be normal or reveal a non-specific soft-tissue mass. Calcification is uncommon. Ultrasound shows a heterogeneous, well-defined, hypoechoic but solid, non-cystic mass with posterior acoustic enhancement (49). CT reveals a well-defined, lobular mass with low attenuation compared with that of skeletal muscle (49). On MRI, the lesion is well-defined and displays low to intermediate signal intensity with lacy, linear, or amorphous high signal intensity foci on T1-weight images and predominantly high signal intensity on T2-weight images (62). Contrast-enhanced MRI typically demonstrates avid heterogeneous enhancement. Histologically, MLS consists of uniform ovoid cells and a variable number of small lipoblasts in a prominent myxoid stroma. Unlike SCL/PL, there is a delicate, arborizing capillary vascular network. DNA damage-inducible transcript 3 (DDIT3) positivity by immunohistochemistry is a sensitive marker for MLS and is expected to be negative in SCL/PL (63). MLS is genetically characterized by a FUS RNA binding protein (*FUS*)-*DDIT3* gene fusion, resulting from a balanced translocation t(12;16)(q13;p11). A variant EWS RNA binding protein 1 (*EWSR1*)-*DDIT3* gene fusion has also been identified in approximately 3% of MLS (61). Detection of these fusion transcripts would be helpful in distinguishing MLS from other adipocytic neoplasms including SCL/PL (64).

DDLS is a malignant adipocytic neoplasm showing transition from ALT to non-lipogenic sarcoma of variable histological grades. It usually presents as a large (>10 cm), painless mass in the retroperitoneum, extremities and paratesticular region. DDLS has a peak incidence in the sixth to seventh decades of life, with no sex predilection (65). Wide excision is the standard treatment for DDLS. Local recurrence occurs in about 40% of cases and distant metastases develop in 15-30% of cases (66). The most important prognostic factor for DDLS is anatomical location. DDLS shares radiological features with ALT or SCL/PL, and dedifferentiation is usually suggested by the presence of a focal, nodular, non-lipomatous region greater than 1cm in size (49). Radiographs may reveal a non-specific soft-tissue mass. Calcification is uncommon. Ultrasound shows a solid, heterogeneous mass with both hypo- and hyperechoic areas (49). CT usually reveals a well-circumscribed, round, or lobulated mass with slightly increased attenuation compared with that of subcutaneous fat in the adipose component and tissue attenuation similar to or slightly lower than that of skeletal muscle in the non-adipose component (67). Contrast-enhanced CT demonstrates definite enhancement in the non-adipose component. MRI typically shows the coexistence of adipose (ALT) and juxtaposed non-adipose (dedifferentiated) components (68, 69). The non-adipose component usually displays low to intermediate signal intensity on T1-weighted images and intermediate to high signal intensity on T2-weighted images. Hemorrhage and necrosis may be seen within the high-grade non-adipose component. Contrast-enhanced MRI demonstrates variable enhancement in the non-adipose component (66). Recently, Parkes *et al*. have suggested that PET/CT is a sensitive and specific diagnostic tool to identify the presence of dedifferentiation within the tumor (70). Histologically, DDLS typically shows an abrupt transition between well-differentiated and dedifferentiated components. The well-differentiated component consists of mature adipocytes with a significant variation in size and atypical, hyperchromatic stromal spindle cells. A varying number of monovacuolated or multivacuolated lipoblasts may be seen. The dedifferentiated component exhibits a wide morphological spectrum but most frequently resemble myxofibrosarcoma or undifferentiated pleomorphic sarcoma (71). Immunohistochemically, diffuse nuclear expression of MDM2 and/or CDK4 is seen in the vast majority of DDLSs. In addition, DDLS shows variable expression of CD34, SMA and desmin (48). The combination of p16 with CDK4 and MDM2 is helpful in distinguishing DDLS from other adipocytic neoplasms including SCL/PL (72). DDLS cytogenetically overlaps with ALT and is characterized by the presence of ring and giant marker chromosomes composed mainly of amplified chromosome 12 sequences (66). Unlike ALT, high-level amplifications of 1p32 and 6q23 are found in DDLS and are associated with a worse prognosis (66). Of note, *MDM2* and/or *CDK4* amplification is typically present in DDLS. DDLS can therefore be distinguished from SCL/PL by FISH for *MDM2* (and/or *CDK4*) amplification.

Conclusion

SCL/PL is a distinctive, benign, adipocytic neoplasm and simple excision is usually curative. The morphologic spectrum of this peculiar neoplasm is surprisingly diverse. SCL/PL should be considered a possible diagnosis when a well-defined, complex, fatty mass is encountered in the subcutis of a middle-aged man. Structural rearrangements, mainly deletions, of 13q are prominent in SCL/PL. Detection of loss of the *RB1* gene would be helpful diagnostically for SCL/PL in selected cases. Further investigations are required to better delineate the relationship between SCL/PL and ASCPLT.

Conflicts of Interest

The Authors declare no conflicts of interest associated with this article.

Authors' Contributions

YO collected the data and searched the literature. JN searched the literature and drafted the article. KK and MA performed the histopathological evaluations. SN and TY reviewed the article. All Authors read and approved the final article.

Acknowledgements

This study was supported in part by the Japan Society for the Promotion of Science KAKENHI (21K09336).

References

1 Billings SD and Ud Din N: Spindle cell lipoma and pleomorphic lipoma. *In*: World Health Organization Classification of Tumours: Soft Tissue and Bone Tumours. Lyon, IARC Press, pp. 29-30, 2020.

2 Fanburg-Smith JC, Devaney KO, Miettinen M and Weiss SW: Multiple spindle cell lipomas: a report of 7 familial and 11 nonfamilial cases. Am J Surg Pathol *22(1)*: 40-48, 1998. PMID: 9422314. DOI: 10.1097/00000478-199801000-00005

3 Ko JS, Daniels B, Emanuel PO, Elson P, Khachaturov V, McKenney JK, Goldblum JR and Billings SD: Spindle cell lipomas in women: a report of 53 cases. Am J Surg Pathol *41(9)*: 1267-1274, 2017. PMID: 28719462. DOI: 10.1097/PAS.0000000000000915

4 Van Treeck BJ and Fritchie KJ: Updates in spindle cell/pleomorphic lipomas. Semin Diagn Pathol *36(2)*: 105-111, 2019. PMID: 30850230. DOI: 10.1053/j.semdp.2019.02.005

5 Braunschweig IJ, Stein IH, Dodwad MI, Rangwala AF and Lopano A: Case report 751: Spindle cell lipoma causing marked bone erosion. Skeletal Radiol *21(6)*: 414-417, 1992. PMID: 1523441. DOI: 10.1007/BF00241825

6 Petit D, Menei P and Fournier HD: An unusual and spectacular case of spindle cell lipoma of the posterior neck invading the spinal cervical canal and posterior cranial fossa. J Neurosurg Spine *15(5)*: 502-506, 2011. PMID: 21819187. DOI: 10.3171/2011.7.SPINE10820

7 Khashper A, Zheng J, Nahal A and Discepola F: Imaging characteristics of spindle cell lipoma and its variants. Skeletal Radiol *43(5)*: 591-597, 2014. PMID: 24554024. DOI: 10.1007/s00256-014-1834-5

8 Choi JW, Kim HJ, Kim J, Kim HJ, Cha JH and Kim ST: Spindle cell lipoma of the head and neck: CT and MR imaging findings. Neuroradiology *55(1)*: 101-106, 2013. PMID: 23053001. DOI: 10.1007/s00234-012-1098-5

9 Younan Y, Martinez A, Reimer N, Edgar M, Gonzalez F, Umpierrez M, Subhawong T and Singer AD: Combined classical spindle cell/pleomorphic lipoma spectrum imaging and clinical data. Skeletal Radiol *47(1)*: 51-59, 2018. PMID: 28823067. DOI: 10.1007/s00256-017-2751-1

10 Bancroft LW, Kransdorf MJ, Peterson JJ, Sundaram M, Murphey MD and O'Connor MI: Imaging characteristics of spindle cell lipoma. AJR Am J Roentgenol *181(5)*: 1251-1254, 2003. PMID: 14573414. DOI: 10.2214/ajr.181.5.1811251

11 Kirwadi A, Abdul-Halim R, Fernando M, Highland A and Kotnis N: MR imaging features of spindle cell lipoma. Skeletal Radiol *43(2)*: 191-196, 2014. PMID: 24240205. DOI: 10.1007/s00256-013-1765-6

12 Jelinek JS, Wu A, Wallace M, Kumar D, Henshaw RM, Murphey MJ, Van Horn A and Aboulafia AJ: Imaging of spindle cell lipoma. Clin Radiol *75(5)*: 396.e15-396.e21, 2020. PMID: 31932047. DOI: 10.1016/j.crad.2019.11.020

13 Kawaguchi M, Kato H, Kobayashi K, Miyazaki T, Nagano A, Noda Y, Hyodo F and Matsuo M: Differences in MRI findings of superficial spindle cell lipoma and atypical lipomatous tumor/well-differentiated liposarcoma. Br J Radiol *96(1143)*: 20220743, 2023. PMID: 36607278. DOI: 10.1259/bjr.20220743

14 Michal M, Kazakov DV, Hadravsky L, Michalova K, Grossmann P, Steiner P, Vanecek T, Renda V, Suster S and Michal M: Lipoblasts in spindle cell and pleomorphic lipomas: a close scrutiny. Hum Pathol *65*: 140-146, 2017. PMID: 28546131. DOI: 10.1016/j.humpath.2017.05.006

15 Billings SD and Folpe AL: Diagnostically challenging spindle cell lipomas: a report of 34 "low-fat" and "fat-free" variants. Am J Dermatopathol *29(5)*: 437-442, 2007. PMID: 17890910. DOI: 10.1097/DAD.0b013e31813735df

16 Hawley IC, Krausz T, Evans DJ and Fletcher CD: Spindle cell lipoma – a pseudoangiomatous variant. Histopathology *24(6)*: 565-569, 1994. PMID: 8063285. DOI: 10.1111/j.1365-2559.1994.tb00577.x

17 Diaz-Cascajo C, Borghi S and Weyers W: Fibrous spindle cell lipoma: report of a new variant. Am J Dermatopathol *23(2)*: 112-115, 2001. PMID: 11285405. DOI: 10.1097/00000372-200104000-00005

18 Wong YP, Chia WK, Low SF, Mohamed-Haflah NH and Sharifah NA: Dendritic fibromyxolipoma: a variant of spindle cell lipoma with extensive myxoid change, with cytogenetic evidence. Pathol Int *64(7)*: 346-351, 2014. PMID: 25047505. DOI: 10.1111/pin.12176

19 Zelger BW, Zelger BG, Plörer A, Steiner H and Fritsch PO: Dermal spindle cell lipoma: plexiform and nodular variants. Histopathology *27(6)*: 533-540, 1995. PMID: 8838333. DOI: 10.1111/j.1365-2559.1995.tb00324.x

20 Chen BJ, Mariño-Enríquez A, Fletcher CD and Hornick JL: Loss of retinoblastoma protein expression in spindle cell/pleomorphic lipomas and cytogenetically related tumors: an immunohistochemical study with diagnostic implications. Am J Surg Pathol *36(8)*: 1119-1128, 2012. PMID: 22790852. DOI: 10.1097/PAS.0b013e31825d532d

21 Nishio J: Contributions of cytogenetics and molecular cytogenetics to the diagnosis of adipocytic tumors. J Biomed Biotechnol *2011*: 524067, 2011. PMID: 21274402. DOI: 10.1155/2011/524067

22 Panagopoulos I, Gorunova L, Lund-Iversen M, Andersen K, Andersen HK, Lobmaier I, Bjerkehagen B and Heim S: Cytogenetics of spindle cell/pleomorphic lipomas: Karyotyping and FISH analysis of 31 tumors. Cancer Genomics Proteomics *15(3)*: 193-200, 2018. PMID: 29695401. DOI: 10.21873/cgp.20077

23 Chen S, Huang H, He S, Wang W, Zhao R, Li L, Cui Z and Zhang R: Spindle cell lipoma: clinicopathologic characterization of 40 cases. Int J Clin Exp Pathol *12(7)*: 2613-2621, 2019. PMID: 31934089.

24 Bartuma H, Nord KH, Macchia G, Isaksson M, Nilsson J, Domanski HA, Mandahl N and Mertens F: Gene expression and

single nucleotide polymorphism array analyses of spindle cell lipomas and conventional lipomas with 13q14 deletion. Genes Chromosomes Cancer *50(8)*: 619-632, 2011. PMID: 21563233. DOI: 10.1002/gcc.20884

25 Uehara K, Ikehara F, Shibuya R, Nakazato I, Oshiro M, Kiyuna M, Tanabe Y, Toyoda Z, Kurima K, Kina S, Hisaoka M and Kinjo T: Molecular signature of tumors with monoallelic 13q14 deletion: a case series of spindle cell lipoma and genetically-related tumors demonstrating a link between FOXO1 status and p38 MAPK pathway. Pathol Oncol Res *24(4)*: 861-869, 2018. PMID: 28887603. DOI: 10.1007/s12253-017-0303-6

26 Mandahl N, Mertens F, Willén H, Rydholm A, Brosjö O and Mitelman F: A new cytogenetic subgroup in lipomas: loss of chromosome 16 material in spindle cell and pleomorphic lipomas. J Cancer Res Clin Oncol *120(12)*: 707-711, 1994. PMID: 7798294. DOI: 10.1007/BF01194267

27 Libbrecht S, Van Dorpe J and Creytens D: The rapidly expanding group of RB1-deleted soft tissue tumors: an updated review. Diagnostics (Basel) *11(3)*: 430, 2021. PMID: 33802620. DOI: 10.3390/diagnostics11030430

28 Hinds B, Agulló Pérez AD, LeBoit PE, McCalmont TH and North JP: Loss of retinoblastoma in pleomorphic fibroma: An immunohistochemical and genomic analysis. J Cutan Pathol *44(8)*: 665-671, 2017. PMID: 28543636. DOI: 10.1111/cup.12965

29 Agaimy A, Michal M, Giedl J, Hadravsky L and Michal M: Superficial acral fibromyxoma: clinicopathological, immunohistochemical, and molecular study of 11 cases highlighting frequent Rb1 loss/deletions. Hum Pathol *60*: 192-198, 2017. PMID: 27825811. DOI: 10.1016/j.humpath.2016.10.016

30 Calo E, Quintero-Estades JA, Danielian PS, Nedelcu S, Berman SD and Lees JA: Rb regulates fate choice and lineage commitment in vivo. Nature *466(7310)*: 1110-1114, 2010. PMID: 20686481. DOI: 10.1038/nature09264

31 Hansen JB, te Riele H and Kristiansen K: Novel function of the retinoblastoma protein in fat: regulation of white versus brown adipocyte differentiation. Cell Cycle *3(6)*: 774-778, 2004. PMID: 15197340.

32 Creytens D and Marino-Enriquez A: Atypical spindle cell lipoma/pleomorphic lipomatous tumour. In: World Health Organization Classification of Tumours: Soft Tissue and Bone Tumours. Lyon, IARC Press, pp. 34-35, 2020.

33 Ichikawa J, Kawasaki T, Imada H, Kanno S, Taniguchi N, Ashizawa T and Haro H: Case report: Atypical spindle cell/pleomorphic lipomatous tumor masquerading as a myxoid liposarcoma or intramuscular myxoma. Front Oncol *12*: 1033114, 2022. PMID: 36439417. DOI: 10.3389/fonc.2022.1033114

34 Sugita S, Sugawara T, Emori M, Aoyama T, Hosaka M, Segawa K, Fujita H and Hasegawa T: Atypical spindle cell/pleomorphic lipomatous tumor with a sarcomatous component showing high mitotic activity and Ki-67 labeling index: report of a unique case mimicking dedifferentiated liposarcoma. Med Mol Morphol *55(4)*: 323-328, 2022. PMID: 35779129. DOI: 10.1007/s00795-022-00327-8

35 Cheng YW, Chen YY, Kuo CH, Liao WC and Kwan AL: Lumbar paraspinal atypical spindle cell/pleomorphic lipomatous tumor: A report of a rare case. Clin Case Rep *11(1)*: e6868, 2023. PMID: 36726691. DOI: 10.1002/ccr3.6868

36 Mariño-Enriquez A, Nascimento AF, Ligon AH, Liang C and Fletcher CD: Atypical spindle cell lipomatous tumor: Clinicopathologic characterization of 232 cases demonstrating a morphologic spectrum. Am J Surg Pathol *41(2)*: 234-244, 2017. PMID: 27879515. DOI: 10.1097/PAS.0000000000000770

37 Creytens D, van Gorp J, Savola S, Ferdinande L, Mentzel T and Libbrecht L: Atypical spindle cell lipoma: a clinicopathologic, immunohistochemical, and molecular study emphasizing its relationship to classical spindle cell lipoma. Virchows Arch *465(1)*: 97-108, 2014. PMID: 24659226. DOI: 10.1007/s00428-014-1568-8

38 Italiano A, Chambonniere ML, Attias R, Chibon F, Coindre JM and Pedeutour F: Monosomy 7 and absence of 12q amplification in two cases of spindle cell liposarcomas. Cancer Genet Cytogenet *184(2)*: 99-104, 2008. PMID: 18617058. DOI: 10.1016/j.cancergencyto.2008.04.004

39 Iwasa Y, Fletcher CDM and Flucke U: Cellular fibroma. In: World Health Organization Classification of Tumours: Soft Tissue and Bone Tumours. Lyon, IARC Press, pp. 80-81, 2020.

40 Figueiredo G, O'Shea A, Neville GM and Lee SI: Rare mesenchymal tumors of the pelvis: Imaging and pathologic correlation. Radiographics *42(1)*: 143-158, 2022. PMID: 34797733. DOI: 10.1148/rg.210049

41 Ntorkou AA, Tsili AC, Giannakis D, Batistatou A, Stavrou S, Sofikitis N and Argyropoulou MI: Magnetic resonance imaging findings of cellular angiofibroma of the tunica vaginalis of the testis: a case report. J Med Case Rep *10*: 71, 2016. PMID: 27029567. DOI: 10.1186/s13256-016-0861-3

42 Iwasa Y and Fletcher CD: Cellular angiofibroma: clinicopathologic and immunohistochemical analysis of 51 cases. Am J Surg Pathol *28(11)*: 1426-1435, 2004. PMID: 15489646. DOI: 10.1097/01.pas.0000138002.46650.95

43 Hameed M, Clarke K, Amer HZ, Mahmet K and Aisner S: Cellular angiofibroma is genetically similar to spindle cell lipoma: a case report. Cancer Genet Cytogenet *177(2)*: 131-134, 2007. PMID: 17854668. DOI: 10.1016/j.cancergencyto.2007.05.016

44 Maggiani F, Debiec-Rychter M, Vanbockrijck M and Sciot R: Cellular angiofibroma: another mesenchymal tumour with 13q14 involvement, suggesting a link with spindle cell lipoma and (extra)-mammary myofibroblastoma. Histopathology *51(3)*: 410-412, 2007. PMID: 17727484. DOI: 10.1111/j.1365-2559.2007.02775.x

45 Flucke U, van Krieken JH and Mentzel T: Cellular angiofibroma: analysis of 25 cases emphasizing its relationship to spindle cell lipoma and mammary-type myofibroblastoma. Mod Pathol *24(1)*: 82-89, 2011. PMID: 20852591. DOI: 10.1038/modpathol.2010.170

46 Panagopoulos I, Gorunova L, Bjerkehagen B, Andersen K, Lund-Iversen M and Heim S: Loss of chromosome 13 material in cellular angiofibromas indicates pathogenetic similarity with spindle cell lipomas. Diagn Pathol *12(1)*: 17, 2017. PMID: 28193293. DOI: 10.1186/s13000-017-0607-6

47 Sbaraglia M, Dei Tos AP and Pedeutour F: Atypical lipomatous tumour/well-differentiated liposarcoma. *In*: World Health Organization Classification of Tumours: Soft Tissue and Bone Tumours. Lyon, IARC Press, pp. 36-38, 2020.

48 Thway K: Well-differentiated liposarcoma and dedifferentiated liposarcoma: An updated review. Semin Diagn Pathol *36(2)*: 112-121, 2019. PMID: 30852045. DOI: 10.1053/j.semdp.2019.02.006

49 Murphey MD, Arcara LK and Fanburg-Smith J: From the archives of the AFIP: imaging of musculoskeletal liposarcoma with radiologic-pathologic correlation. Radiographics *25(5)*: 1371-1395, 2005. PMID: 16160117. DOI: 10.1148/rg.255055106

50 Nishio J, Iwasaki H, Nabeshima K, Kamachi Y and Naito M: Atypical lipomatous tumor with structural rearrangements

involving chromosomes 3 and 8. Anticancer Res *34(6)*: 3073-3076, 2014. PMID: 24922675.
51 Demicco MG, Fritchie KJ and Han A: Solitary fibrous tumor. In: World Health Organization Classification of Tumours: Soft Tissue and Bone Tumours. Lyon, IARC Press, pp. 104-108, 2020.
52 Martin-Broto J, Mondaza-Hernandez JL, Moura DS and Hindi N: A comprehensive review on solitary fibrous tumor: new insights for new horizons. Cancers (Basel) *13(12)*: 2913, 2021. PMID: 34200924. DOI: 10.3390/cancers13122913
53 Wignall OJ, Moskovic EC, Thway K and Thomas JM: Solitary fibrous tumors of the soft tissues: review of the imaging and clinical features with histopathologic correlation. AJR Am J Roentgenol *195(1)*: W55-W62, 2010. PMID: 20566782. DOI: 10.2214/AJR.09.3379
54 Papathanassiou ZG, Alberghini M, Picci P, Staals E, Gambarotti M, Garaci FG and Vanel D: Solitary fibrous tumors of the soft tissues: imaging features with histopathologic correlations. Clin Sarcoma Res *3(1)*: 1, 2013. PMID: 23351922. DOI: 10.1186/2045-3329-3-1
55 Nishio J, Iwasaki H, Aoki M, Nabeshima K and Naito M: FDG PET/CT and MR imaging of CD34-negative soft-tissue solitary fibrous tumor with NAB2-STAT6 fusion gene. Anticancer Res *35(2)*: 967-971, 2015. PMID: 25667482.
56 Nielsen GP, Dickersin GR, Provenzal JM and Rosenberg AE: Lipomatous hemangiopericytoma. A histologic, ultrastructural and immunohistochemical study of a unique variant of hemangiopericytoma. Am J Surg Pathol *19(7)*: 748-756, 1995. PMID: 7793472. DOI: 10.1097/00000478-199507000-00002
57 Thway K, Ng W, Noujaim J, Jones RL and Fisher C: The current status of solitary fibrous tumor: diagnostic features, variants, and genetics. Int J Surg Pathol *24(4)*: 281-292, 2016. PMID: 26811389. DOI: 10.1177/1066896915627485
58 Cheah AL, Billings SD, Goldblum JR, Carver P, Tanas MZ and Rubin BP: STAT6 rabbit monoclonal antibody is a robust diagnostic tool for the distinction of solitary fibrous tumour from its mimics. Pathology *46(5)*: 389-395, 2014. PMID: 24977739. DOI: 10.1097/PAT.0000000000000122
59 Robinson DR, Wu YM, Kalyana-Sundaram S, Cao X, Lonigro RJ, Sung YS, Chen CL, Zhang L, Wang R, Su F, Iyer MK, Roychowdhury S, Siddiqui J, Pienta KJ, Kunju LP, Talpaz M, Mosquera JM, Singer S, Schuetze SM, Antonescu CR and Chinnaiyan AM: Identification of recurrent NAB2-STAT6 gene fusions in solitary fibrous tumor by integrative sequencing. Nat Genet *45(2)*: 180-185, 2013. PMID: 23313952. DOI: 10.1038/ng.2509
60 Fritchie KJ, Carver P, Sun Y, Batiouchko G, Billings SD, Rubin BP, Tubbs RR and Goldblum JR: Solitary fibrous tumor: is there a molecular relationship with cellular angiofibroma, spindle cell lipoma, and mammary-type myofibroblastoma? Am J Clin Pathol *137(6)*: 963-970, 2012. PMID: 22586056. DOI: 10.1309/AJCPQEG6YNN6CNAL
61 Thway K and Nielsen TO: Myxoid liposarcoma. In: World Health Organization Classification of Tumours: Soft Tissue and Bone Tumours. Lyon, IARC Press, pp. 42-44, 2020.
62 Saifuddin A, Andrei V, Rajakulasingam R, Oliveira I and Seddon B: Magnetic resonance imaging of trunk and extremity myxoid liposarcoma: diagnosis, staging, and response to treatment. Skeletal Radiol *50(10)*: 1963-1980, 2021. PMID: 33792747. DOI: 10.1007/s00256-021-03769-w
63 Scapa JV, Cloutier JM, Raghavan SS, Peters-Schulze G, Varma S and Charville GW: DDIT3 immunohistochemistry is a useful tool for the diagnosis of myxoid liposarcoma. Am J Surg Pathol *45(2)*: 230-239, 2021. PMID: 32815829. DOI: 10.1097/PAS.0000000000001564
64 Iwasaki H, Ishiguro M, Nishio J, Aoki M, Yokoyama R, Yokoyama K, Taguchi K and Nabeshima K: Extensive lipoma-like changes of myxoid liposarcoma: morphologic, immunohistochemical, and molecular cytogenetic analyses. Virchows Arch *466(4)*: 453-464, 2015. PMID: 25650275. DOI: 10.1007/s00428-015-1721-z
65 Dei TOS AP, Marino-Enriquez A and Pedeutour F: Dedifferentiated liposarcoma. In: World Health Organization Classification of Tumours: Soft Tissue and Bone Tumours. Lyon, IARC Press, pp. 39-41, 2020.
66 Nishio J, Nakayama S, Nabeshima K and Yamamoto T: Biology and management of dedifferentiated liposarcoma: state of the art and perspectives. J Clin Med *10(15)*: 3230, 2021. PMID: 34362013. DOI: 10.3390/jcm10153230
67 Hong SH, Kim KA, Woo OH, Park CM, Kim CH, Kim MJ, Chung JJ, Han JK and Rha SE: Dedifferentiated liposarcoma of retroperitoneum: spectrum of imaging findings in 15 patients. Clin Imaging *34(3)*: 203-210, 2010. PMID: 20416485. DOI: 10.1016/j.clinimag.2009.12.025
68 Nishio J, Aoki M, Nabeshima K, Iwasaki H and Naito M: Cytogenetic and molecular cytogenetic findings in giant dedifferentiated liposarcoma of the thigh. Oncol Rep *27(3)*: 764-768, 2012. PMID: 22160092. DOI: 10.3892/or.2011.1584
69 Nishio J, Iwasaki H, Nabeshima K and Naito M: Immunohistochemical, cytogenetic, and molecular cytogenetic characterization of both components of a dedifferentiated liposarcoma: implications for histogenesis. Anticancer Res *35(1)*: 345-350, 2015. PMID: 25550570.
70 Parkes A, Urquiola E, Bhosale P, Lin H, Watson K, Wang WL, Feig B, Torres K, Roland CL, Conley AP, Zarzour M, Livingston JA, Ratan R, Ludwig J, Araujo DM, Ravi V, Benjamin RS, Patel S and Somaiah N: PET/CT imaging as a diagnostic tool in distinguishing well-differentiated versus dedifferentiated liposarcoma. Sarcoma *2020*: 8363986, 2020. PMID: 32565716. DOI: 10.1155/2020/8363986
71 Mori T, Yamada Y, Kinoshita I, Kohashi K, Yamamoto H, Ito Y, Susuki Y, Kawaguchi K, Nakashima Y and Oda Y: Clinicopathological and histopathological review of dedifferentiated liposarcoma: a comprehensive study of 123 primary tumours. Histopathology *80(3)*: 538-557, 2022. PMID: 34699612. DOI: 10.1111/his.14588
72 Thway K, Flora R, Shah C, Olmos D and Fisher C: Diagnostic utility of p16, CDK4, and MDM2 as an immunohistochemical panel in distinguishing well-differentiated and dedifferentiated liposarcomas from other adipocytic tumors. Am J Surg Pathol *36(3)*: 462-469, 2012. PMID: 22301498. DOI: 10.1097/PAS.0b013e3182417330

Received March 14, 2023
Revised March 29, 2023
Accepted April 4, 2023